Inorg. Chem. **1999,** *38,* 4249−4255

Derivation of Force Field Parameters, and Force Field and Quantum Mechanical Studies of Layered α- and γ-Zirconium Phosphates

Giulio Alberti,[†] Antonio Grassi,[‡] Giuseppe M. Lombardo,[‡] Giuseppe C. Pappalardo,*,[‡] and Riccardo Vivani[†]

Dipartimento di Chimica, Università di Perugia, Via Elce di Sotto 8, 06123 Perugia, Italy, and
Dipartimento di Scienze Chimiche, Università di Catania, Cattedra di Chimica Generale,
Facoltà di Farmacia, Viale A. Doria 6, 95125 Catania, Italy

Received April 9, 1999

A set of force field (FF) parameters was derived for bonds and atoms of the uncommon structural units (Zr−O; O−Zr−O; Zr−O−P; etc.) in layered α- and γ-zirconium phosphates (α- and γ-ZrP). To accomplish this parametrization we relied on the technique of energy derivatives obtained from ab initio quantum mechanics on a model compound as outlined by Dinur and Hagler. To check the reliability of the derived FF parameters the crystal structures of α- and γ-ZrP were calculated using the Open Force Field routine of Cerius^2. The computed results were compared with the experimental X-ray crystal structures and also with the energy results obtained from the CRYSTAL95 program that performs quantum mechanical calculations on periodic systems. The discrepancies between the FF optimized structures and the experimental structures for α- and γ-ZrP were quite acceptable. The unit cells attained differences smaller than 6% (β angle of the γ-ZrP cell), while for the valence coordinate the maximum root-mean-square deviation values were 0.03 Å for the bond distances (P−O in γ-ZrP), and 5.82° for the bond angles (Zr−O−P in α-ZrP). The CRYSTAL95 calculated energies (per zirconium phosphate unit) using as input the experimental X-ray structure, and the FF optimized geometry, showed small differences. The ΔE values (1.26 and 3.26 kcal mol^{-1}, for α- and γ-ZrP, respectively, in favor of the X-ray geometry) does not rule out the population of both experimental and FF structures. Furthermore, their calculated electronic characteristics were analogous. Finally, comparisons made using vibrational spectroscopy data as benchmarks showed that calculated vibrational bands were in acceptable agreement with experiments.

Introduction

The chemistry of lamellar materials has grown considerably in the last thirty years. These materials are of great interest due to some important applications in different areas of science and technology such as ion exchange, intercalation, and catalysis.[1,2] By linking adjacent layers with inorganic or organic pillars, even micro- and mesoporous solids can be prepared.[3−7] 2D-nanochemistry in the interlayer space can be extended to include a wide range of nanoscale device applications.[8−10]

Unfortunately, many layered compounds are obtained only as powders, often of low crystallinity, thus making difficult or impossible structural determinations by X-ray analysis. The availability of synchrotron and neutron sources has favored, in recent years, a rapid development of experimental and numerical techniques for structure determination (not only Rietveld refinement) from powder diffraction data making possible their application even to systems of medium complexity.[8,11] However, even in cases where the lamellar solids initially exhibit a high degree of crystallinity, overlapping large bands from relatively poor diffraction patterns are often observed when these solids are modified by ion-exchange, intercalation, pillaring, or topotactic functionalization by ligand substitution. Thus, detailed structural information on these derivatives is difficult to extract from their diffraction patterns.

The force field (FF) technique is a powerful tool for investigating large polyatomic molecular systems. Such a technique could be applied to layered systems of this type when the lack of crystallinity prevents unambiguous information from X-ray diffraction methods. Furthermore, the availability of a suitable FF allows the application of molecular dynamics (MD) simulations. Within the framework of the MD scheme it is possible to (i) monitor internal molecular fluctuations, (ii)

---

* To whom correspondence should be addressed. Fax: 39 075 5855566. E-mail: alberti@unipg.it.

[†] Università di Perugia.

[‡] Università di Catania.

(1) Alberti, G. In *Solid-State Supramolecular Chemistry: Two- and Three-Dimensional Inorganic Networks*; Alberti, G., Bein T., Eds.; Comprehensive Supramolecular Chemistry Series; Pergamon: Oxford, 1996; Vol. 7, Chapter 5.

(2) Clearfield, A.; Costantino, U. In *Solid-State Supramolecular Chemistry: Two- and Three-Dimensional Inorganic Networks*; Alberti, G., Bein T., Eds.; Comprehensive Supramolecular Chemistry Series; Pergamon: Oxford, 1996; Chapter 4 and references therein.

(3) Alberti, G.; Costantino, U.; Vivani, R.; Zappelli, P. *Angew. Chem., Int. Ed. Engl.* **1993**, *32*, 1357.

(4) Alberti, G.; Marmottini, F.; Murcia-Mascarós, S.; Vivani, R. *Angew. Chem., Int. Ed. Engl.* **1994**, *33*, 1594.

(5) Alberti, G.; Vivani, R.; Marmottini, F.; Zappelli, P. *J. Porous Mater.* **1998**, *5*, 205.

(6) Alberti, G.; Marmottini, F.; Vivani, R.; Zappelli, P. *J. Porous Mater.* **1998**, *5*, 221.

(7) Clearfield, A. In *Design of New Materials*; Cocke, D. L., Clearfield, A., Eds.; Plenum Press: New York, 1987; p 121.

(8) Clearfield, A. In *Progress in Inorganic Chemistry*; Karlin, K. D., Ed.; John Wiley & Sons: New York, 1998; Vol. 47, p 374.

(9) Yang, H. C.; Aoki, K.; Hong, H. G.; Sackett, D. D.; Arrendt, M. F.; Yau, S. L.; Bell, C. M.; Mallouk, T. E. *J. Am. Chem. Soc.* **1993**, *115*, 11855.

(10) Alberti, G.; Casciola, M.; Costantino, U.; Vivani, R. *Adv. Mater.* **1996**, *8*, 291.

(11) Alberti, G.; Vivani, R.; Murcia-Mascarós, S. *J. Mol. Struct.* **1998**, *469*, 81.

10.1021/ic9903937 CCC: $18.00

generate microscopic-level information, (iii) explore wide portions of the conformational space, and (iv) help the interpretation of X-ray diffraction data for low-crystallinity solids. Among the main advantages provided by MD simulations there is the possibility to reveal functional properties for homologous or congeneric series, and to find correlation with experimentally detectable macroscopic properties through the judicious use of statistical mechanics.

Accordingly, the MD implemented with a FF is well suited to describe the dynamic properties of the system. The results of these calculations can also provide insights into the heights of conformational barriers and into the population probability density of each relative minimum in the entire conformational space. Such information in lamellar systems cannot be achieved using X-ray analysis.

Conformational changes of the intercalated molecules associated with interlayer distance variations are also very important for understanding pillaring, intercalation and supramolecular chemistry in interlayer spaces of the lamellar compounds. Thus, the application of the FF techniques could be particularly suitable for the study of lamellar materials, their intercalates and/or their organic derivatives. However, the use of FF techniques for lamellar systems requires a suitable set of parameters for all the internal coordinates of the uncommon structural units in these materials.

To test the effective potentiality, we apply the above techniques to two well investigated lamellar zirconium phosphates: the zirconium bis-monohydrogen phosphate (α-$Zr(O_3POH)_2 \cdot H_2O$, hereafter α-ZrP); and the zirconium phosphate dihydrogenphosphate (γ-$ZrPO_4H_2PO_4 \cdot 2H_2O$, hereafter γ-ZrP). The structures of these lamellar compounds have been established since 1964[12,13] and 1990,[14,15] respectively. Both α-ZrP and γ-ZrP are of considerable interest, not only for their applications,[1−7] but also because a large variety of organic derivatives has been prepared from these hosts.[8−10,16,17] These derivatives can be considered as two very large and versatile classes of layered materials in which many different geometrical arrangements can be realized by an appropriate choice of the organic group covalently bonded to α- or γ-inorganic layers. They also include α- and γ-ZrP covalently pillared by rigid organic groups[3,4,17] which find important applications in the field of tailor-made molecular sieves,[18,19] shape selective catalysis,[7] and layer-by-layer growth of ultrathin films.[9] Of particular interest are also some derivatives pillared with nonrigid groups in which the interlayer distance depends on the length, conformational properties, and relative flexibility of the organic pillars.[20] When long alkyl chains are used as pillars, considerable elongation and shortening of the interlayer distance, in an accordion-like movement, has been observed. Since pillaring often causes a severe loss of crystallinity, the use of X-ray diffraction remains essentially limited to the determination of the interlayer changes. Also in this case, MD simulations could be useful for providing detailed insights about structural and conformational changes that take place owing to the accordion effect.

To derive FF parameters for layered α- and γ-ZrP we rely on the technique of energy derivatives obtained from ab initio quantum mechanics on a model compound as outlined by Dinur and Hagler.[21] Then, to check the reliability of the FF parameters here derived, the FF calculated crystal structures of α- and γ-ZrP were compared with the X-ray crystal data,[12−15] vibrational spectroscopy,[22] as well as with energetic results obtained from quantum chemical calculations. These latter calculations were performed with the CRYSTAL95 program[23] using as input atomic coordinates coming from the FF calculated structure and then from the experimental crystal structures of both α- and γ-ZrP. The CRYSTAL95 calculations should also provide insight into the electronic features of these materials that are also reported here.

Computational Methods

The GAUSSIAN94 program[24] was used for the quantum chemical ab initio at the Hartree−Fock level calculations needed for obtaining second derivatives of the energy. The split-valence 3-21G* basis set contained in this program was selected. The use of this basis set is actually necessary being the most sophisticated “all electrons” basis among those including the Zr atom. Since relativistic effects are reported to be significant only for heavier atoms,[25,26] these terms were not taken into account in the calculations.

The Cerius^2 package[27] was used for application of the FF techniques to crystalline materials by imposing periodic boundary conditions through the crystal builder and the Open Force Field routines.

The ground-state energies of the crystals of α- and γ-ZrP were calculated using the CRYSTAL95 package.[23] This program, within the HF-LCAO approximation, allows the calculation of the wave functions and correlated properties of crystalline systems. In the present work all the calculations were performed using a Pople standard STO-4G basis set for hydrogen and oxygen atoms. For P and Zr atoms, the ECP (effective core potential) approximation was introduced with the HAYWLC (Hay and Wadt large core) basis set.

Protocols of the FF Calculations. The new parameters developed in this work were created for use with the Universal Force Field through the Open Force Field routine in Cerius^2.[28]

Periodic conditions were imposed in the Cerius^2 FF calculations for the zirconium phosphates. The scale factor for the nonbond (NB) 1−4 interactions was set to 0.5.[29] The NB interactions cutoff was implemented according to the SPLINE method as a function of the interatomic distance values (r) as follows: for $r <$ SPLINE-ON $=$ 20.0 Å, fully considered; for $r >$ SPLINE-OFF $=$ 25.0 Å, fully ignored; for SPLINE-ON $< r <$ SPLINE-OFF, reduced in magnitude. The dielectric constant in the electrostatic function was set as $\epsilon = 1$; the

---

(12) Clearfield, A.; Stynes, J. A. *J. Inorg. Nucl. Chem.* **1964**, *26*, 117.
(13) Troup, J. M.; Clearfield, A. *Inorg. Chem.* **1977**, *16*, 3311.
(14) Christensen, A.; Andersen, E. K.; Andersen, I. G. K.; Alberti, G.; Nielsen, N.; Lehmann, M. S. *Acta Chem. Scand.* **1990**, *44*, 865.
(15) Poojary, D. M.; Shpeizer, B.; Clearfield, A. *J. Chem. Soc., Dalton Trans.* **1995,** 111.
(16) Alberti, G.; Costantino, U.; Allulli, S.; Tomassini, N. *J. Inorg. Nucl. Chem.* **1978**, *40*, 1113.
(17) Alberti, G.; Boccali, L.; Dionigi, C.; Vivani, R.; Kalchenko, V. I. *Supramol. Chem.* **1998**, *9*, 99.
(18) Dines, M. B.; Di Giacomo, P. M. *Inorg. Chem.* **1981**, *20*, 92.
(19) Clearfield, A. *Comments Inorg. Chem.* **1990**, *10*, 283.
(20) Alberti, G.; Murcia-Mascarós, S.; Vivani, R. *J. Am. Chem. Soc.* **1998**, *120*, 9291.
(21) Dinur, U.; Hagler, A. T. In *Reviews in Computational Chemistry*; Lipkowitz, K. B., Boyd, D. B., Eds.; VCH Publishers: New York, 1991; Vol. 2, p 99.
(22) Slade, C. T.; Knowles, J. A.; Jones, D. J.; Rozière, J. *Solid State Ionics* **1997**, *96*, 9.
(23) Dovesi, R.; Saunders, V. R.; Roetti, C.; Causà, M.; Harrison, N. M.; Orlando, R.; Aprà, E. *CRYSTAL95 User’s Manual*; University of Torino: Torino, Italy, 1996.
(24) Frisch, M. J.; Trucks, G. W.; Schlegel, H. B.; Gill, P. M. W.; Johnson, B. G.; Robb, M. A.; Cheeseman, J. R.; Keith, T.; Petersson, G. A.; Montgomery, J. A.; Raghavachari, K.; Al-Laham, M. A.; Zakrzewski, V. G.; Ortiz, J. V.; Foresman, J. B.; Cioslowski, J.; Stefanov, B. B.; Nanayakkara, A.; Challacombe, M.; Peng, C. Y.; Ayala, P. Y.; Chen, W.; Wong, M. W.; Andres, J. L.; Replogle, E. S.; Gomperts, R.; Martin, R. L.; Fox, D. J.; Binkley, J. S.; Defrees, D. J.; Baker, J.; Stewart, J. P.; Head-Gordon, M.; Gonzalez, C.; Pople, J. A. *Gaussian 94*, Revision C.3; Gaussian, Inc.: Pittsburgh, PA, 1995.
(25) Pitzer, K. S. *Acc. Chem. Res.* **1979**, *12*, 271.
(26) Ziegler, T.; Snijders, J. G.; Baerends, E. J. *J. Chem. Phys.* **1981**, *74*, 1271.
(27) Cerius^2 program package developed by BIOSYM/MSI.
(28) Rappe, A. K.; Casewit, C. J.; Colwell, K. S.; Goddard, W. A., III; Skiff, W. M. *J. Am. Chem. Soc.* **1992**, *114*, 10024.
(29) Weiner, P. K.; Kollman, P. A. *J. Comput. Chem.* **1981**, *2*, 287.

Table 1. Universal Force Field[a] Set of Parameters for Zirconium Phosphates[b]

parameter	l_0 (Å)	k_s (kcal mol^{-1} Å^{-2})	α_0 (deg)	k_b (kcal mol^{-1} deg^{-2})	l_0 (Å)	k_{UB} (kcal mol^{-1} Å^{-2})	k_ϕ (kcal mol^{-1})	n	ϕ_0
Zr−O	2.0646	171.66							
P−O	1.5300	700.00							
O−Zr−O			90.00	149.23	2.920	128.60			
(O−Zr−O)			180.00	8.74	4.130	90.90			
Zr−O−P			150.81	169.45	3.460	251.34			
O−P−O			109.47	140.24	2.500	96.07			
P−O−H			112.82	104.92	2.000	81.68			
Zr−O−P−O							20.930	1	0.0
							0.750	2	0.0
							0.116	3	0.0
O−Zr−O−P							9.732	1	0.0
							2.836	2	0.0
							0.790	3	0.0
(O−Zr−O)−P							0.0[c]	1	0.0
O−P−O−H							12.920	1	0.0
							3.210	2	0.0
							0.008	3	0.0

[a] Reference 28. [b] The default values of the universal force field are valid for the remaining parameters not quoted in the table. [c] The (O−Zr−O)−P torsional angle is neglected because of the (O−Zr−O) bond angle of 180°.

atomic charges were calculated by the Charge Equilibration[30] routine; the energy minimization used the Conjugate Gradient 200 method, up to a gradient of 0.1 kcal mol^{-1} Å^{-1}.

The Cerius^2 package does not allow carrying out vibrational normal-mode analysis. Therefore the velocity auto-correlation function (VACF) (eq 1) method, as implemented in the Cerius^2, was used to calculate the vibrational frequencies of both α- and γ-ZrP.

$$g(\tau) = \lim_{T\to\infty}\frac{1}{T}\int_0^T \nu(t)\,\nu(t+\tau)\mathrm{d}t \tag{1}$$

The Fourier transform of the VACF gives the power spectrum. In the power spectrum the position of each peak corresponds to a frequency of the vibrational motions of the system.

While this type of analysis does not distinguish between the various types of normal modes (stretching, scissoring, etc.), it does provide information about the vibrational frequencies of corresponding peaks in the power spectrum of the selected atom or group of atoms.

The above vibrational analysis uses the atomic velocities that are attainable from MD simulations performed for a single cell. The following MD settings were used: (i) integration time step 0.001 ps; (ii) total number of run steps 30 000 (30 ps); (iii) snapshots (of the velocity) every 4 steps (0.004 ps). The power spectrum was calculated in the frequency range of about 4000 cm^{-1} with interval steps of about 1 cm^{-1}. The FF settings remained unchanged.

The CONSTANT NPT (constant pressure, temperature) method of MD was used with a T_DAMPING[31] thermostat; the relaxation time was set to 0.100 ps, and the mass pre-factor to 1.0. The pressure and the temperature were set at 0.00 GPa and 298 K, respectively.

Determination of the FF Parameters. The FF parameters were developed for zirconium phosphates using our previously described procedure[32] based on the method of energy derivative[21] from ab initio calculations on model compounds. Such an analytical method for calculating the force constants has been successfully applied to phosphazenic compounds[32,33] for which the FF parameters were calculated for use in MM2 and CHARMm programs.

The method is based on the assumption that the ab initio and the FF calculated potential energy surfaces have the same shape, and thus $E_{QM} = E_{FF} + K$ with $K =$ constant. Accordingly the derivatives at a given point will have the same value in both ab initio and FF cases.

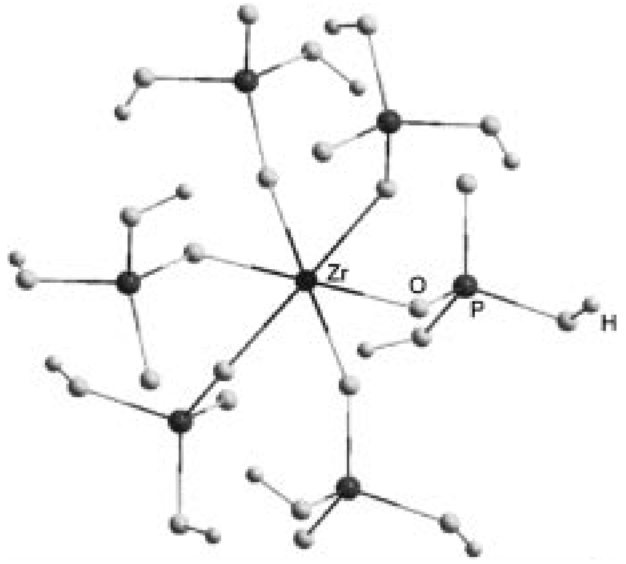

Figure 1. Perspective view of the model compound $Zr(H_2PO_4)_6^{2-}$.

A remarkable feature of the energy derivative is that it allows deletion of the undesired energy terms so that we may attain each calculated term completely pure from the other interactions (see the Appendix). This makes the parameters transferable from one chemical environment to another, independent of the attached substituents, and thus is suited for application to layered zirconium phosphates.

This procedure requires calculation of the quantum mechanical energy, and of its derivatives. These calculations were performed using the GAUSSIAN94 program (3-21G* level) on the model compound $Zr(H_2PO_4)_6^{2-}$ (Figure 1) having an octahedral Zr atom. The model compound was built up along the Hopfinger−Pearlstein guideline.[34] According to this guideline, either α-ZrP or γ-ZrP produces the same model compound. Since the differences between bond distances and angles of the two different α and γ structures are negligible, the calculations were performed, without geometry optimization, on the model (−2 charged) built up on the basis of the γ-ZrP geometry.

The values of the ab initio calculated energy second derivative depend on the specific valence coordinate. Therefore, the value of a given force constant K_A was the mean of the calculated values of the specific type of bond length and bond angle in the model molecule.

As a first step, the equilibrium values of each bond (l_0) and angle (α_0) were assumed to be the mean value for the specific type of bond

---

(30) Rappe, A. K.; Goddard, W. A., III. *J. Phys. Chem.* **1991**, *95*, 3358.

(31) Berendsen, H. J.; Postma, J. P. O.; Van Gunsteren, W. I.; Di Nola, A.; Haak, J. R. *J. Chem. Phys.* **1984**, *81*, 3684.

(32) Amato, M. E.; Lipkowitz, K. B.; Lombardo, G. M.; Pappalardo, G. C. *J. Mol. Struct.* **1995**, *372*, 69.

(33) Caminiti, R.; Gleria, M.; Lipkowitz, K. B.; Lombardo, G. M.; Pappalardo, G. C. *J. Am. Chem. Soc.* **1997**, *119*, 2196.

(34) Hopfinger, A. J.; Pearlstein, R. A. *J. Comput. Chem.* **1984**, *5*, 486.

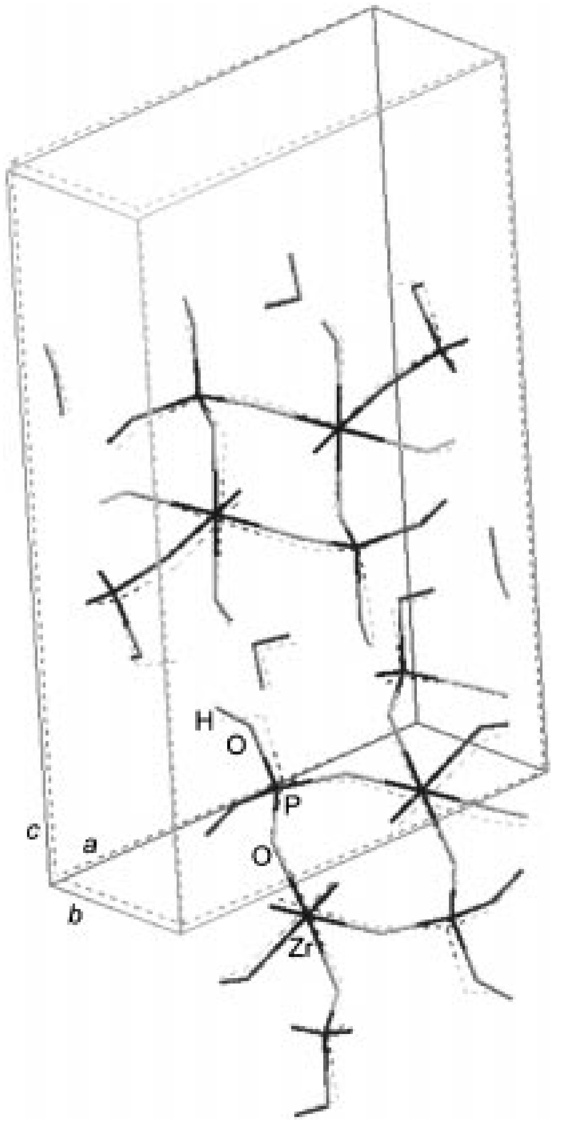

Figure 2. Graphic comparison by superposition of the FF calculated (dot line) and X-ray determined (solid line) structures of α-ZrP.

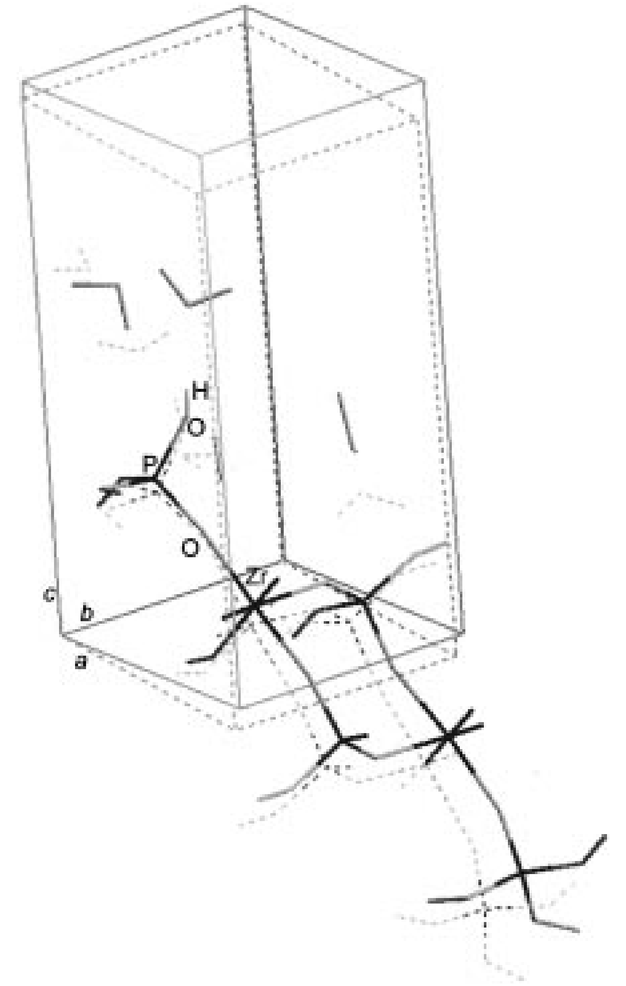

Figure 3. Graphic comparison by superposition of the FF calculated (dot line) and X-ray determined (solid line) structures of γ-ZrP.

Table 2. Comparison of FF-Calculated Unit Cell Constants with Experimental Crystal Data[13,15] for α-ZrP and γ-ZrP

	α-ZrP		γ-ZrP	
	X-ray	FF	X-ray	FF
space group	$P2_1/n$		$P2_1$	
a (Å)	9.060	8.895	5.383	5.302
b (Å)	5.297	5.151	6.634	6.566
c (Å)	15.414	15.435	12.410	12.051
α (deg)	90.000	90.002	90.000	90.035
β (deg)	101.71	100.904	98.687	104.514
γ (deg)	90.000	90.002	90.000	90.044

length and bond angle in the calculated structure. Successively the final values for l_0 and α_0 parameters were obtained by test and trial refinement of these values to minimize the differences between the experimental and FF calculated crystal structure of γ-ZrP. The torsional parameters were derived using the same model compound and the energy second derivative with respect to the torsion angle procedure described in detail by Dinur and Hagler.[35]

Results and Discussion

The calculated FF parameter set for zirconium phosphates is given in Table 1. The validity of these parameters was checked first by comparison between FF calculated and experimental geometries,[12-15] vibrational spectroscopy data,[22] and quantum mechanical calculations (CRYSTAL95) as benchmarks.

The unit cells of α- and γ-ZrP attained using FF optimizations were in good agreement with those coming from X-ray diffraction experiments (Table 2). The maximum difference between the FF optimized and experimental unit cells is less than 5%. This result is outlined in a comparative fashion by Figures 2 and 3.

The comparisons between FF optimized and experimental geometries of α- and γ-ZrP are shown in Tables 3 and 4, respectively. The Open Force Field routine of Cerius^2 does not allow structure optimization under symmetry constraint so that all the atoms inside the unit cell were explicitly considered in the calculations. Accordingly, in Tables 3 and 4 each experimental value of bond distance and angle is matched to four FF calculated values in the case of α-ZrP (due to its $P2_1/n$ symmetry) and to two FF calculated values for γ-ZrP ($P2_1$ symmetry), respectively.

For the sake of easy comparison, Tables 3 and 4 quote the average values of the FF calculated geometric data. These average values were also used for calculating the root-mean-square deviation (rmsd) compared to the experimental values for each type of structural unit in the zirconium phosphates.

The data in Table 5 indicate that the discrepancies between the FF optimized and the experimental structures are acceptable. The rmsd values attained a maximum of 0.03 Å for the P−O

---

(35) Dinur, U.; Hagler, A. T. *J. Comput. Chem.* **1990**, *11*, 1234.

Table 3. Comparison of FF Results with the Experimental X-ray Data for Structural Features of α-ZrP

	FF[a]				FF[b]	X-ray[c]		FF[a]				FF[b]	X-ray[c]
Zr−O(4)	2.044	2.044	2.044	2.044	**2.044**	**2.048**	P(2)−O(4)	1.518	1.518	1.518	1.518	**1.518**	**1.510**
Zr−O(5)	2.053	2.054	2.054	2.054	**2.054**	**2.074**	P(2)−O(5)	1.519	1.519	1.519	1.519	**1.519**	**1.512**
Zr−O(6)	2.057	2.058	2.058	2.058	**2.058**	**2.071**	P(2)−O(6)	1.523	1.523	1.523	1.523	**1.523**	**1.524**
Zr−O(8)	2.047	2.047	2.048	2.047	**2.047**	**2.054**	P(2)−O(7)	1.524	1.524	1.524	1.524	**1.524**	**1.564**
Zr−O(9)	2.050	2.050	2.051	2.050	**2.050**	**2.065**	P(3)−O(8)	1.519	1.519	1.519	1.519	**1.519**	**1.517**
Zr−O(11)	2.051	2.052	2.052	2.052	**2.052**	**2.075**	P(3)−O(9)	1.521	1.521	1.521	1.521	**1.521**	**1.518**
							P(3)−O(10)	1.521	1.521	1.521	1.521	**1.521**	**1.551**
							P(3)−O(11)	1.521	1.521	1.521	1.521	**1.521**	**1.519**
O(4)−Zr−O(5)	91.1	91.1	91.1	91.1	**91.1**	**91.14**	O(4)−P(2)−O(5)	109.5	109.5	109.5	109.5	**109.5**	**112.4**
O(4)−Zr−O(6)	90.4	90.4	90.4	90.4	**90.4**	**90.45**	O(4)−P(2)−O(6)	107.7	107.6	107.7	107.6	**107.7**	**110.5**
O(4)−Zr−O(8)	89.2	89.2	89.2	89.2	**89.2**	**89.76**	O(4)−P(2)−O(7)	109.7	109.7	109.7	109.7	**109.7**	**109.2**
O(4)−Zr−O(9)	88.7	88.6	88.7	88.7	**88.7**	**89.35**	O(5)−P(2)−O(6)	108.7	108.8	108.8	108.8	**108.8**	**111.4**
O(4)−Zr−O(11)	179.4	179.4	179.4	179.4	**179.4**	**178.85**	O(5)−P(2)−O(7)	110.6	110.7	110.7	110.7	**110.7**	**103.6**
O(5)−Zr−O(6)	88.7	88.6	88.6	88.6	**88.6**	**88.96**	O(6)−P(2)−O(7)	110.5	110.5	110.5	110.5	**110.5**	**109.6**
O(5)−Zr−O(8)	90.7	90.7	90.7	90.7	**90.7**	**88.88**	O(8)−P(3)−O(9)	108.7	108.6	108.7	108.7	**108.7**	**110.6**
O(5)−Zr−O(9)	179.7	179.7	179.7	179.7	**179.7**	**179.51**	O(8)−P(3)−O(10)	110.1	110.2	110.1	110.1	**110.1**	**109.2**
O(5)−Zr−O(11)	89.3	89.2	89.2	89.2	**89.2**	**89.96**	O(8)−P(3)−O(11)	109. 1	109.0	109.0	109.0	**109.0**	**111.4**
O(6)−Zr−O(8)	179.2	179.1	179.2	179.2	**179.2**	**177.83**	O(9)−P(3)−O(10)	110. 4	110.5	110.5	110.5	**110.5**	**109.8**
O(6)−Zr−O(9)	91.2	91.2	91.2	91.2	**91.2**	**91.04**	O(9)−P(3)−O(11)	108.2	108.2	108.2	108.2	**108.2**	**111.0**
O(6)−Zr−O(11)	89.2	89.2	89.1	89.1	**89.1**	**89.91**	O(10)−P(3)−O(11)	110.3	110.3	110.3	110.4	**110.4**	**104.7**
O(8)−Zr−O(9)	89.5	89.5	89.5	89.5	**89.5**	**91.12**							
O(8)−Zr−O(11)	91.2	91.2	91.2	91.2	**91.2**	**89.92**							
O(9)−Zr−O(11)	91.0	91.0	91.0	91.0	**91.0**	**89.55**							
Zr−O(4)−P(2)	149.7	149.7	149.6	149.6	**149.7**	**160.6**	Zr−O(8)−P(3)	149.0	149.0	149.0	149.0	**149.0**	**157.5**
Zr−O(5)−P(2)	148.1	148.1	148.1	148.1	**148.1**	**145.4**	Zr−O(9)−P(3)	148.3	148.3	148.3	148.3	**148.3**	**149.4**
Zr−O(6)−P(2)	146.4	146.4	146.5	146.5	**146.5**	**146.1**	Zr−O(11)−P(3)	147.5	147.5	147.5	147.5	**147.5**	**145.8**

[a] Four values for each bond distance and bond angle structural unit corresponding to the four symmetry positions ($P2_1/n$). [b] Average value of the four FF values. [c] Reference 13.

Table 4. Comparison of FF Results with Experimental X-ray Data for Structural Features of γ-ZrP

	FF[a]		FF[b]	X-ray[c]		FF[a]		FF[b]	X-ray[c]
Zr−O(4)	2.057	2.059	**2.058**	**2.028**	Zr−O(7)	2.056	2.056	**2.056**	**2.032**
Zr−O(5)	2.045	2.034	**2.040**	**2.059**	Zr−O(8)	2.072	2.073	**2.073**	**2.086**
Zr−O(6)	2.033	2.047	**2.040**	**2.026**	Zr−O(9)	2.065	2.059	**2.062**	**2.014**
P(2)−O(4)	1.517	1.516	**1.517**	**1.571**	P(3)−O(8)	1.528	1.529	**1.529**	**1.545**
P(2)−O(5)	1.523	1.522	**1.523**	**1.527**	P(3)−O(9)	1.530	1.526	**1.528**	**1.545**
P(2)−O(6)	1.522	1.525	**1.524**	**1.531**	P(3)−O(10)	1.532	1.530	**1.531**	**1.586**
P(2)−O(7)	1.534	1.534	**1.534**	**1.568**	P(3)−O(11)	1.533	1.534	**1.534**	**1.545**
O(4)−Zr−O(5)	89.5	87.0	**88.3**	**89.7**	O(5)−Zr−O(9)	91.1	89.1	**90.1**	**91.2**
O(4)−Zr−O(6)	88.3	90.8	**89.6**	**85.6**	O(6)−Zr−O(7)	87.8	88.5	**88.2**	**95.7**
O(4)−Zr−O(7)	93.0	93.0	**93.0**	**95.8**	O(6)−Zr−O(8)	90.8	92.9	**91.9**	**87.3**
O(4)−Zr−O(8)	85.7	85.6	**85.7**	**84.3**	O(6)−Zr−O(9)	91.4	93.4	**92.4**	**93.2**
O(4)−Zr−O(9)	174.1	172.7	**173.4**	**174.8**	O(7)−Zr−O(8)	178.5	177.5	**178.0**	**177.6**
O(5)−Zr−O(6)	176.1	176.1	**176.1**	**173.5**	O(7)−Zr−O(9)	92.8	93.1	**93.0**	**89.3**
O(5)−Zr−O(7)	88.3	89.1	**88.7**	**89.8**	O(8)−Zr−O(9)	88.5	88.5	**88.5**	**90.6**
O(5)−Zr−O(8)	92.3	92.9	**92.6**	**87.9**					
O(4)−P(2)−O(5)	108.2	109.9	**109.1**	**109.4**	O(8)−P(3)−O(9)	108.5	108.3	**108.4**	**110.4**
O(4)−P(2)−O(6)	111.5	109.6	**110.6**	**109.8**	O(8)−P(3)−O(10)	106.3	107.1	**106.7**	**108.2**
O(4)−P(2)−O(7)	107.0	106.9	**107.0**	**104.3**	O(8)−P(3)−O(11)	111.1	110.6	**110.9**	**109.1**
O(5)−P(2)−O(6)	109.9	110.2	**110.1**	**113.5**	O(9)−P(3)−O(10)	112.0	111.4	**111.7**	**109.4**
O(5)−P(2)−O(7)	109.9	111.5	**110.7**	**110.0**	O(9)−P(3)−O(11)	111.4	111.6	**111.5**	**109.6**
O(6)−P(2)−O(7)	110.2	108.6	**109.4**	**109.4**	O(10)−P(3)−O(11)	107.4	107.7	**107.6**	**110.0**
Zr−O(4)−P(2)	160.3	160.4	**160.4**	**161.7**	Zr−O(7)−P(3)	147.6	147.7	**147.7**	**153.1**
Zr−O(5)−P(2)	146.0	147.1	**146.6**	**145.6**	Zr−O(8)−P(3)	144.1	143.8	**144.0**	**145.8**
Zr−O(6)−P(2)	147.3	145.6	**146.5**	**144.9**	Zr−O(9)−P(3)	154.4	157.3	**155.9**	**164.3**

[a] Two values for each bond distance and bond angle structural unit corresponding to the two symmetry positions ($P2_1$). [b] Average value of the two FF values. [c] Reference 15.

bond distances in γ-ZrP, and of 5.82° for the Zr−O−P bond angles in α-ZrP. It is relevant that the higher rmsd value pertains to a bond angle that in the experimental structure ranges from 145.4° to 160.6° for α-ZrP (Table 3), and from 144.9° to 164.3° for γ-ZrP (Table 4). The same trend occurs for the O−P−O angles, although in this case the range of variation of the experimental values (about 9°) is not as large in both α- and γ-ZrP and the rmsd values are lower than those attained for the Zr−O−P angle. The discrepancies between experimental and FF calculated bond angles might therefore be correlated to the degree of variability of these angles in the crystals. Such wide variations of bond angles for the same type of atoms cannot be reproduced so accurately by the FF technique. This is because of the inherent limitation of the assumed harmonic function used for calculating the bond angle potential energy term (that otherwise gives high energy for wide excursions of the angle about the equilibrium value).

The VACF calculated power spectra reproduced the features observed in the range 1055−964 cm^{-1}, and at 591 and 540 cm^{-1}, assigned to vibrational modes of the hydrogen phosphate

Table 5. Root Mean Square Deviations (rmsd) of the FF-Calculated Averaged Values for Each Type of Bond Distance (Å) and Bond Angle (deg) of α-ZrP and γ-ZrP from X-ray Crystal Data

	rmsd	
	α-ZrP	γ-ZrP
Zr−O	0.0152	0.0274
P−O	0.0181	0.0313
O−Zr−O	0.967	3.24
O−P−O	3.23	1.92
Zr−O−P	5.82	4.25

Table 6. Relative Energies (kcal mol^{-1}) of α- and γ-ZrP Calculated by FF and Quantum Mechanical (QM) Methods[a]

	FF	QM
α-ZrP·H_2O	−18.515	1.44
γ-ZrP·$2H_2O$	−48.608	3.26

[a] The energy values are relative to the corresponding energies calculated for the X-ray geometries and assumed as 0.0.

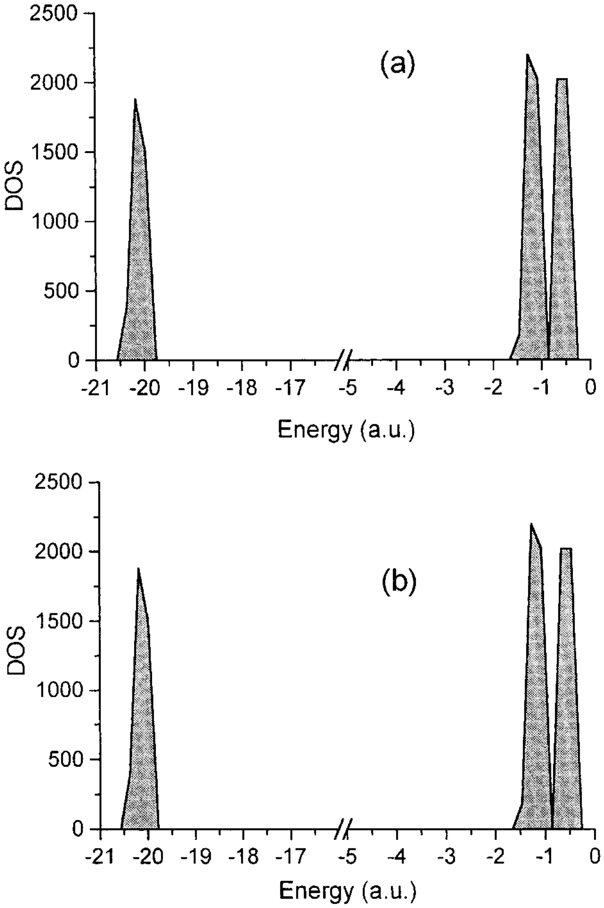

Figure 4. Valence density of states (DOS) for the FF calculated (a) and X-ray determined (b) structures of α-ZrP.

groups in the layers of α-ZrP.[22] The frequencies at 399, 1250, and 1401 cm^{-1} featuring the HPO_4^{2-} species[22] were also attained by the FF calculated power spectra, thus indicating reliability of the derived force constants.

In Table 6 are reported the total energies (per zirconium phosphate unit) calculated by FF, and those calculated by CRYSTAL95 using as input atomic coordinates from the X-ray study and from the FF optimized structures. The results revealed that the quantum mechanically calculated energies favor by a small extent (1.26 and 3.26 kcal mol^{-1} for α- and γ-ZrP, respectively) the experimental structures with respect to the FF optimized ones.

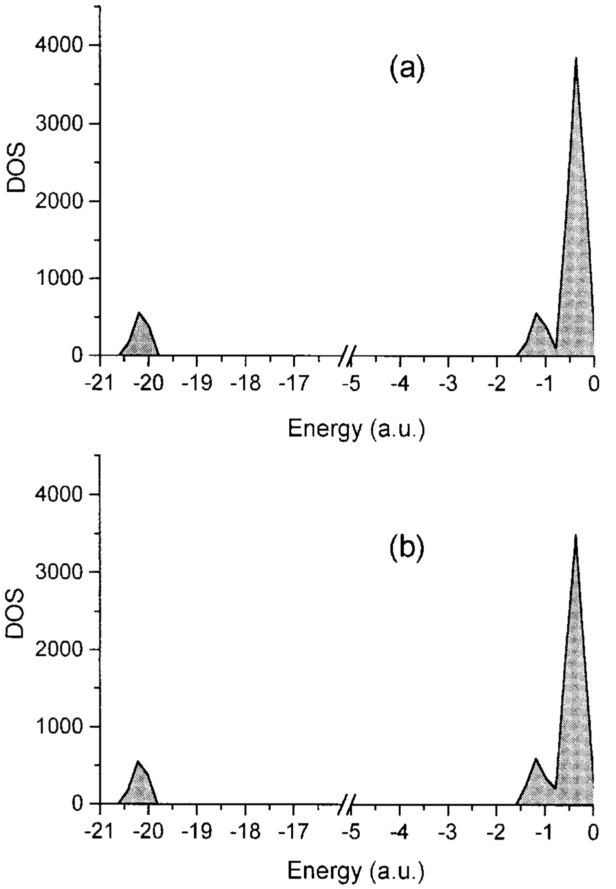

Figure 5. Valence density of states (DOS) for the FF calculated (a) and X-ray determined (b) structures of γ-ZrP.

Table 7. Fermi Energy (ϵ_F, au) for the FF and X-ray Structures of α- and γ-ZrP; Differences ($\Delta\epsilon_F$, au) also Quoted

	FF	X-ray	$\Delta\epsilon_F$
α-ZrP·H_2O	−0.2133	−0.2042	−0.0091
γ-ZrP·$2H_2O$	−0.1568	−0.1660	0.0092

The electronic features calculated by CRYSTAL95 are scarcely affected on passing from the X-ray to the FF calculated geometry. In fact, the densities of states of both X-ray and FF structures were almost the same (Figures 4 and 5). The values of the Fermi levels ϵ_F) (Table 7) show that the differences between the levels attained using the FF and X-ray geometry are ca. 0.25 eV for both α-ZrP and γ-ZrP.

Conclusions

In this paper we carried out quantum mechanical calculations on a model system to derive parameters for use with the Universal Force Field. The results obtained confirm that the FF technique indeed provides reliable results for layered zirconium phosphates. It is therefore plausible to suppose that useful insights into the structural properties of other layered materials, through inclusion of ad hoc developed set of parameters, can also be obtained. The implementation we attained of FF technique will now allow us to perform FF calculations, MD simulations, and molecular modeling of lamellar zirconium phosphates. This set of FF parameters is found to be suitable for studies focusing on structural, energetic, and dynamic features of intercalation compounds in general and, in particular, of pillared derivatives of layered zirconium phosphates.

The application of this technique is also particularly promising for providing insights into the structural properties of low-crystallinity lamellar systems or their derivatives that cannot be studied by X-ray techniques.

Appendix

The total energy of the molecule in the FF calculation can be written as (eq A1):

$$E = E_s + E_b + E_{UB} + E_{tor} + E_{nb} = \sum V_s(b) + \sum V_b(\theta) + \sum V_{UB}(l) + \sum V_{tor}(\phi) + \sum V_{nb}(r) \quad (A1)$$

in which the energy terms are represented by V_s (bond stretching), V_b (bending), V_{UB} (Urey−Bradley), V_{nb} (nonbonded), and V_{tor} (torsional). The energy first derivative with respect to the *i*th atom position is then

$$\frac{\partial E^{QM}}{\partial r_i} = \frac{\partial E^{FF}}{\partial r_i} = \frac{\partial V_s(b_i)}{\partial r_i} + \frac{\partial}{\partial r_i}\sum_{kj} V_b(\theta_{ijk}) + \frac{\partial}{\partial r_i}\sum_{k} V_{UB}(l_{ik}) + \frac{\partial}{\partial b_i}\sum_{m} V_{nb}(r_{im}) + \frac{\partial}{\partial r_i}\sum_{jkl} V_{tor}(\phi_{ijkl}) \quad (A2)$$

while the second derivative with respect to the position of atoms *i* and *j* (with atom *i* bonded to atom *j*) is

$$\frac{\partial^2 E^{QM}}{\partial r_i \partial r_j} = \frac{\partial^2 E^{FF}}{\partial r_i \partial r_j} = \frac{\partial^2 V_s(b_i)}{\partial r_i \partial r_j} + \frac{\partial^2}{\partial r_i \partial r_j}\sum_{k} V_b(\theta_{ijk}) + \frac{\partial^2}{\partial r_i \partial r_j}\sum_{k,l} V_{tor}(\phi_{ijkl}) \quad (A3)$$

Equations A2 and A3 show that increasing the order of the energy derivative will decrease the number of terms contributing to its value.

Equation A3 represents the off-diagonal elements of the Cartesian Hessian matrix for atoms *i* and *j* and is related to the interactions between these two atoms purified from the other energy terms.

Acknowledgment. Paper supported by “Fondi MURST ex-40% 1997−1999”.

IC9903937